



## Joule heating during flash-sintering

Rishi Raj\*

*Department of Mechanical Engineering, University of Colorado at Boulder, Boulder, CO 80309-0427, United States*

Received 18 November 2011; received in revised form 12 February 2012; accepted 20 February 2012

Available online 15 March 2012

### Abstract

Flash-sintering is invariably accompanied by a highly non-linear rise in the specimen's conductivity. Thus the specimen temperature rises above the furnace temperature. It is shown that flash-sintering is a transient phenomenon, where the power dissipation rises quickly at first, but then declines towards a steady state, as the power supply switches from voltage to current control. The area under the power spike, which is equal to the Joules expended in the sample during the transient, is absorbed by the heat capacity of the specimen. Therefore, the specimen temperature rises gradually towards this steady state through the transient. Whereas the power spike can exceed a peak value of  $1000 \text{ mW mm}^{-3}$ , the dissipation during the current controlled regime is in the  $100\text{--}400 \text{ mW mm}^{-3}$  range. The extrapolation of sintering time from a few hours, as in conventional sintering, to a few seconds, using the activation energy for diffusion, predicts sample temperatures that are far in excess of the measured specimen temperature during flash sintering.

© 2012 Elsevier Ltd. All rights reserved.

**Keywords:** Sintering; Flash-sintering; Field assisted sintering

### 1. Introduction

In flash-sintering a powder preform sinters abruptly above a threshold condition. This transition is prescribed by a combination of the furnace-temperature and the DC electrical field applied directly to the specimen by a pair of electrodes. This phenomenon occurs in several oxide systems, including yttria stabilized zirconia,<sup>1,2</sup> magnesia doped alumina,<sup>3</sup> strontium titanate,<sup>4</sup> cobalt manganese oxide,<sup>2</sup> titania (unpublished) and magnesium-aluminate spinel (unpublished). A characteristic feature of this process is that the sudden onset of sintering is accompanied by an equally abrupt increase in the conductivity of the specimen. Immediately the power supply must be switched to current control so as to prevent electrical runaway. In current control the power expended in the specimen declines since the resistance of the specimen continues to fall. The specimen temperature rises gradually through the power-spike towards a quasi-steady state value in this current controlled regime.

The extent of the rise in the specimen temperature is an important first step towards understanding the mechanism of flash-sintering. Higher temperature implies higher diffusion rate

of mass transport. The temperature required to sinter in a just a few seconds can be extrapolated from the conventional time and temperature through the activation energy for diffusion. The question is whether or not the specimen temperature reaches this extrapolated value as a result of Joule heating.

There have been at least two attempts to estimate the specimen temperature as a function of power dissipation. In one instance, the specimen temperature was obtained by measuring the thermal expansion as a function of power input.<sup>5</sup> In the other case the temperature was estimated by a numerical simulation.<sup>6</sup> It is important to note that in both cases, power was applied to the specimen at a constant rate until a steady state was reached.

The temperature of the specimen during transient power, as in flash sintering, has also been measured,<sup>7</sup> and is much lower than would be estimated assuming the peak power to be applied to the specimen at a constant rate.

The following sections are divided into three major parts: (a) Joule heating for steady state power dissipation, (b) the transient case of flash sintering, and (c) estimate of the specimen temperature that would be required to sinter yttria stabilized zirconia in just a few seconds, which is then compared to the specimen temperature discussed in the previous sections.

The flash-sintering experiments can be divided into two categories: sinterforging where a field as well as a uniaxial stress is applied to the specimen,<sup>5,7</sup> and free, two electrode experiments

\* Corresponding author. Tel.: +1 303 492 1029; fax: +1 303 492 3498.

E-mail address: [rishi.raj@colorado.edu](mailto:rishi.raj@colorado.edu)

where the electrical field is applied to the ends of an otherwise unconstrained specimen.<sup>1–4</sup>

The experiments that are discussed below were carried out on yttria-doped zirconia: 3YSZ<sup>1,7</sup> and 8YSZ.<sup>5</sup>

## 2. Case I: steady state power dissipation

This section is divided into three subsections. In the first, a model for Joule heating based upon black body radiation is described. These results are presented in the form of maps that allow a quick estimate of the specimen temperature from the knowledge of the furnace temperature, the steady-state power dissipation, and the surface to volume ratio of the specimen. In the next two sections experimental<sup>5</sup> and numerical simulation<sup>6</sup> data are compared with the black body radiation model.

### 2.1. Black body radiation model for joule heating

If a sample initially at the furnace temperature,  $T_0$ , is heated electrically then the rise in its temperature, to  $T$ , relative to  $T_0$ , can be estimated by assuming that the difference in the black body radiation at  $T$  and  $T_0$  is equal to the heat dissipated within the sample. This approach assumes that convection and conduction losses into the environment are negligible. Black body radiation increases as  $T^4$ , therefore it is greater than the convection losses above about 800 °C (at dull red color). The conduction losses, however, depend greatly on the electrode and system configuration and, therefore, cannot be estimated generally.

The estimate for  $T$  was analyzed in an earlier paper for small rise in the sample temperature. It is derived in Ref. 9, which expressed in incremental form becomes:

$$\frac{\delta T}{T} = \frac{\delta W}{4A\sigma T^4} \quad (1)$$

Integrating Eq. (1) between the limits of 0 to  $W$ , as sample temperature rises from  $T_0$  to  $T$ , leads to the following equation:

$$T = \left[ T_0^4 + \frac{W}{A\sigma} \right]^{1/4} \quad (2)$$

In Eq. (2),  $\sigma = 5.67 \times 10^{-8} \text{ W m}^2 \text{ K}^{-4}$  is a universal physical constant,  $A$  is the surface area of the sample in  $\text{m}^2$ ,  $W$  is the electrical energy dissipated in the sample in  $\text{W}$ , and the temperature is expressed in  $\text{K}$ . Eq. (2) assumes the emissivity of the ceramic to be unity; indeed for most oxides its value is greater than 0.9. Later, the discrepancy between theory and experiment is tied to this assumption: a true emissivity that is less than one would give higher specimen temperatures than calculated here.

The surface area of the sample,  $A$ , depends on the sample geometry. It is useful to normalize  $W$  with respect to the volume of the sample, written here as  $V$ , so that:

$$W_V = \frac{W}{V} \quad (3)$$

where  $W_V$  is in units of  $\text{W m}^{-3}$ .

Eq. (2) can now be rewritten in normalized form as follows:

$$\frac{T}{T_0} = \left[ 1 + \frac{W_V}{\sigma T_0^4} \left( \frac{V}{A} \right) \right]^{1/4} \quad (4)$$

Note that  $V/A$  is the volume to surface ratio, with units of  $\text{m}$ .

It can be more convenient to write  $W_V$  in units of  $\text{mW mm}^{-3}$ , and  $V/A$  in units of  $\text{mm}$ , in which case Eq. (4) becomes:

$$\left\{ \frac{T}{T_0} = \alpha \left[ 1 + \frac{1000 W_V (\text{mW mm}^{-3})}{\sigma T_0^4} \left( \frac{V}{A} (\text{mm}) \right) \right]^{1/4} \right\} \quad (5)$$

where the units for the key parameters are shown in brackets.  $\alpha$  is a correction factor to account for the fact that the emissivity of the sample is less than unity; therefore  $\alpha \geq 1$ , with  $\alpha$  being greater than one if the emissivity is less than unity. The predictions from Eq. (5) are mapped in Fig. 1, with the assumption that  $\alpha = 1$ . The power dissipation and the furnace temperature are the axes. Knowing these two parameters, the estimate of the specimen temperature can be read quickly. Since the results depend on the volume to surface area ratio, four maps for  $(V/A) = 0.5, 0.75, 1.0, \text{ and } 2.0 \text{ mm}$  are given. For example, if the furnace temperature is 1100 °C, then in order to reach a specimen temperature of 1450 °C, a power density of 600  $\text{mW mm}^{-3}$  would be required for  $(V/A) = 0.5 \text{ mm}$ , or 150  $\text{mW mm}^{-3}$  if  $(V/A) = 2.0 \text{ mm}$ , and so on. The predictions from Eq. (5) are compared to experiments and a numerical simulation in the next section.

In the following sections we shall find that Eq. (5) underestimates the specimen temperature by 100–200 °C, most likely because the oxide has an emissivity that is less than unity.

### 2.2. Comparison with numerical simulation<sup>6</sup>

Soon after the publication of flash-sintering in 3YSZ zirconia,<sup>1</sup> Grasso et al.<sup>6</sup> repeated the experiment and sought to explain the phenomenon in terms of Joule heating by numerical simulation. Their specimen geometry was approximately the same as in Ref. 1, that is a rectangular gage section, 21 mm long with a cross section of 3 mm × 1.58 mm, which gives  $(V/A) = 0.52 \text{ mm}$ . In the simulation they assumed a (steady state) power dissipation of 70 W which corresponds to 700  $\text{mW mm}^{-3}$ , and a furnace temperature of  $T_0 = 850 \text{ °C}$ . The reading from Fig. 1, marked as point (A), predicts a specimen temperature of 1400 °C. The simulation gave a range of temperatures in the specimen, with the highest value reaching 1600 °C. The underestimate is attributed to the emissivity of the specimen being less than unity.

### 2.3. Comparison with experimental results<sup>5</sup>

Baraki et al.<sup>5</sup> have measured the temperature of a 95% dense sample of 8YSZ as a function of the power dissipated in the specimen. The sample was a cylindrical piece, 8 mm in diameter and 4 mm tall, which gives  $(V/A) = 1.0 \text{ mm}$ . The furnace temperature was,  $T_0 = 1200 \text{ °C}$ . The specimen temperature was estimated from volumetric thermal expansion. These

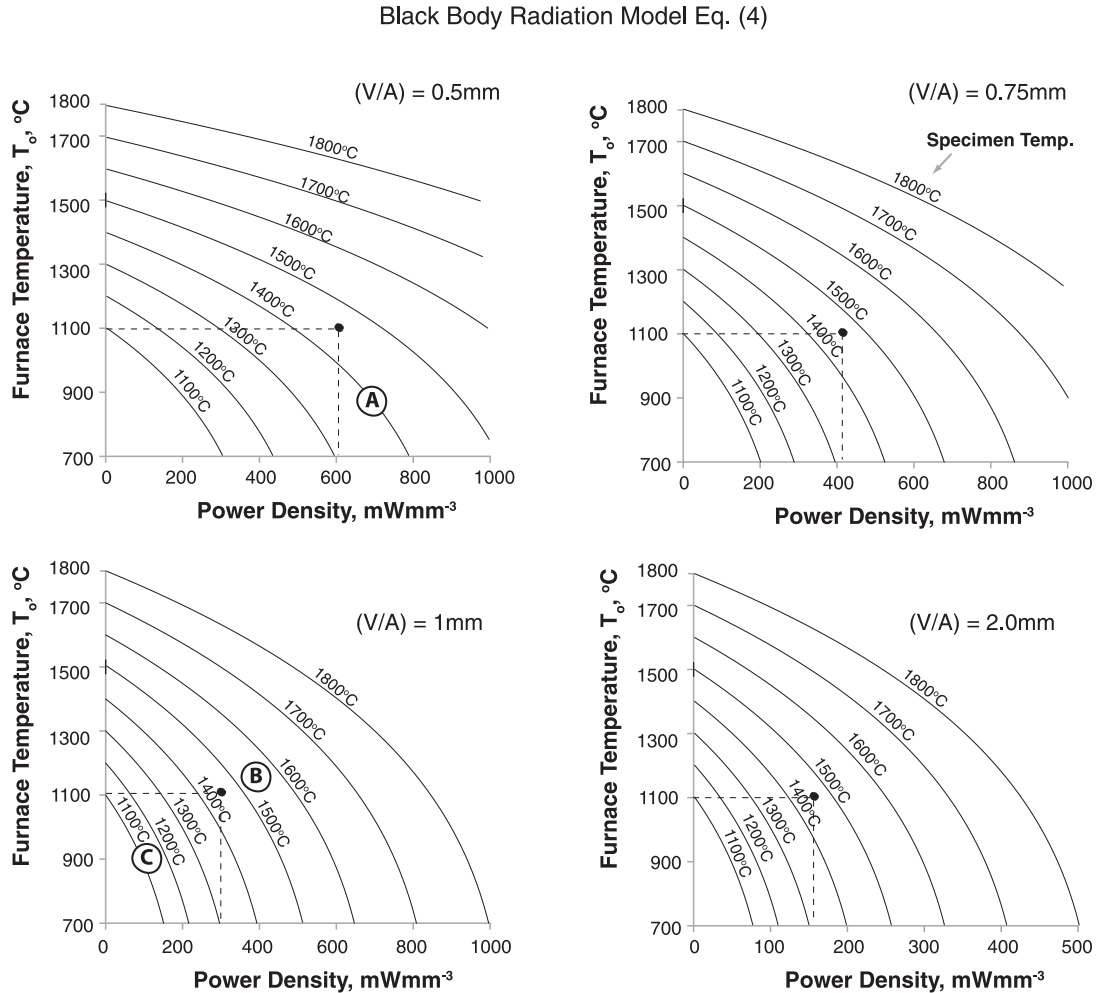


Fig. 1. Maps for estimating the specimen temperature given the furnace temperature and the power dissipation in the specimen for four different values of the volume-to-surface ratio ( $V/A$ ). The points A, B and C are from a simulation and experiments. A is from a simulation,<sup>6</sup> B from steady state power dissipation,<sup>5</sup> and C from flash-sinterforging experiment.<sup>7</sup> The model is based upon black body radiation, as given by Eq. (4).

measurements are compared with the prediction of the furnace temperature, from Eq. (5), in Fig. 2. In this instance, the agreement is reasonably fair with the model underestimating the specimen temperature by approximately 100°C at a power level of 400 mW mm<sup>-3</sup>, as shown by the point (B) in Fig. 1.

### 3. Case II: flash-sintering, the transient case

In this section we discuss Joule heating during a flash-sintering experiment. In our laboratory, so far, these experiments have been carried out by first applying a constant dc electric field to the specimen, and then ramping the furnace temperature at a rate of 10 °C min<sup>-1</sup>. The current in the specimen rises abruptly at a threshold value of the temperature. The power supply is quickly switched from voltage control to current control upon reaching a preset value of the current. The power to the specimen then falls sharply since its conductivity continues to increase, before settling down to a quasi-steady state level. The power-vs.-time curve, therefore shows a spike with an effective width of about 1 s. The question that is addressed in the

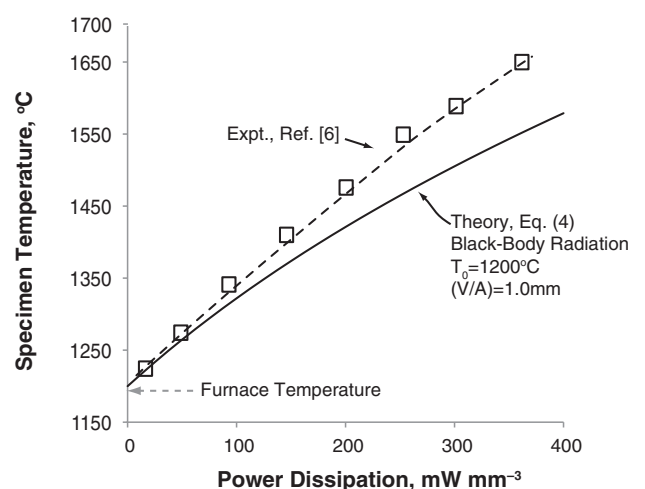


Fig. 2. A comparison of the black body radiation model with experiments under steady state power dissipation in the specimen while the furnace temperature is held constant at 1250 °C.<sup>5</sup>

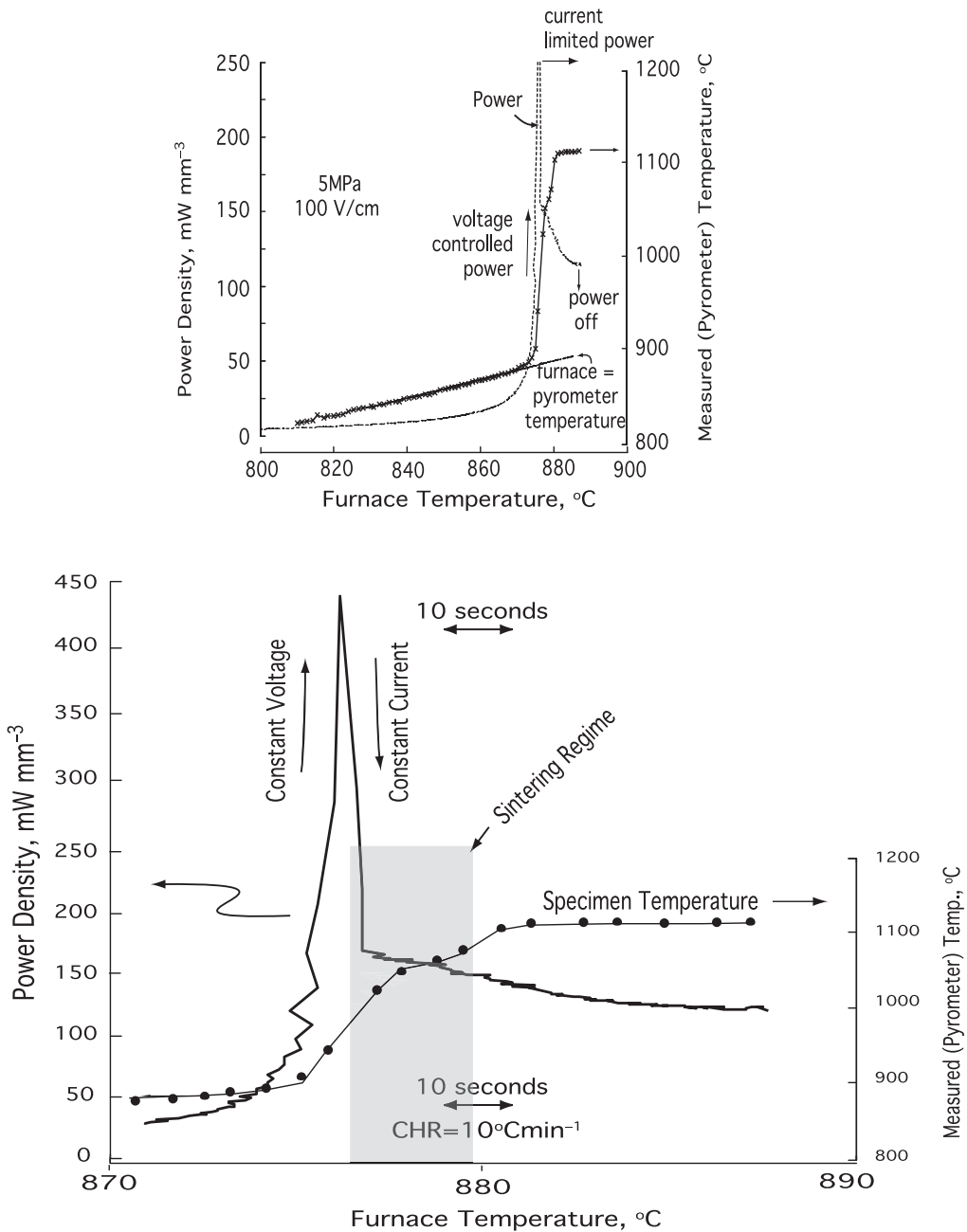


Fig. 3. The relationship between the power-density and the specimen temperature in the time domain, in a flash-sinterforging experiment.<sup>7</sup>

following sections is how the power dissipation is related to the specimen temperature, in the time domain.

This section is divided into two sub-sections. The first considers flash sinterforging of cylindrical specimens under a uniaxial load. The second considers flash sintering of unconstrained dog-bone shaped specimens.

### 3.1. Flash sinterforging of 3YSZ

A typical set of results from a sinterforging experiment is given in Fig. 3. In this experiment a load of 5 MPa and a field equal to  $100 \text{ V cm}^{-1}$  were applied. The furnace was then heated at a constant rate of  $10 \text{ }^{\circ}\text{C min}^{-1}$ . The onset of flash sintering

took place when the furnace temperature was approximately  $875 \text{ }^{\circ}\text{C}$ . The samples were of a cylindrical shape with a diameter of 5 mm and 10 mm long, giving a value  $(V/A) = 0.75 \text{ mm}$  (considering only the bare surface of the cylinder).

The temperature of the specimen was measured by focusing a pyrometer on its surface. The pyrometer had been previously calibrated with a dense 3YSZ sample placed within a furnace (without applying electrical field) and then raising the furnace temperature in steps up to  $1400 \text{ }^{\circ}\text{C}$ .

The upper graph in Fig. 3 shows the power density, and the specimen temperature. It spans a range from  $800 \text{ }^{\circ}\text{C}$  to  $900 \text{ }^{\circ}\text{C}$ . Note that the furnace temperature and the pyrometer temperature agree perfectly until the onset of the power surge, when the

specimen temperature begins to outpace the furnace temperature. Upon reaching a power density of  $450 \text{ mW mm}^{-3}$  the power supply was switched from voltage control to current control. The power into the specimen immediately begins to decline. Meanwhile the temperature of the specimen continues to increase, through the transient, finally approaching a steady state. At this point the power dissipation in the specimen also approaches a quasi-steady state.

An expanded view of the data spanning  $870\text{--}890^\circ\text{C}$  is given in the lower half of Fig. 3. The power density immediately falls after spiking at  $450 \text{ mW mm}^{-3}$ , declining to  $250 \text{ mW mm}^{-3}$  in less than 2 s. Gradually, both the power and the temperature approach a steady state such that a specimen temperature of  $1125^\circ\text{C}$  is achieved at a power density of  $125 \text{ mW mm}^{-3}$ . This measurement is shown as point (C) in the maps in Fig. 1. In this case, the experimental and the calculated temperatures are in fair agreement.

In Section 4 we will estimate how high the temperature must rise above the conventional sintering temperature in order to achieve sintering in just a few seconds.

### 3.2. Flash sintering experiments without uniaxial load

Unconstrained flash-sintering experiments in our laboratory have been carried out with dog-bone shaped specimens, suspended into a conventional furnace with two platinum wires that also serve as the electrodes to supply electric field and current to the specimen. The field is applied before the furnace is ramped up at  $10^\circ\text{C min}^{-1}$ . The gage section of the specimens is 21 mm long with a rectangular cross section of  $1.58 \text{ mm} \times 3.0 \text{ mm}$ . Explicit details of the method are given in Ref. 3.

In all instances the power-time plot has the same shape as shown in Fig. 3 for the sinterforging experiment. (The graphs in the publications<sup>1–4</sup> are somewhat misleading since they only show the peak value of the power spike but not its shape in expanded time domain.)

A typical result from these experiments, in this instance with 3YSZ, is shown in Fig. 4. It shows the flash regime spanning a total time of 30 s, during which period the furnace temperature rises from  $905^\circ\text{C}$  to  $910^\circ\text{C}$ . In this instance the current was limited to  $40 \text{ mA mm}^{-2}$ . The lower graph gives the power-profile, and the upper plot shows the sintering profile. It is to be noted that the power spike is less than 1 s. The steady state power dissipation, which is achieved in current control is about one half the peak value, at approximately  $200 \text{ mW mm}^{-3}$ .

The DC field required to induce flash sintering varies greatly from one material to another. For example in the case of YSZ the range is from  $30 \text{ V cm}^{-1}$  to  $120 \text{ V cm}^{-1}$ . In MgO-doped alumina the field can be as high as  $1000 \text{ V cm}^{-1}$ , while in the case of cobalt-manganese oxide it is much smaller, about  $12.5 \text{ V cm}^{-1}$ . Yet in all instances the peak value of the power dissipation is nearly the same. The quasi-steady state power in the current control regime usually approaches one half of the peak value, and lies in the  $100\text{--}400 \text{ mW mm}^{-3}$  range. Therefore, the current limit set in the experiments is highly variable. For example, while it was  $\sim 40 \text{ mA mm}^{-2}$  for 3YSZ, it was only  $\sim 12 \text{ mA mm}^{-2}$  for

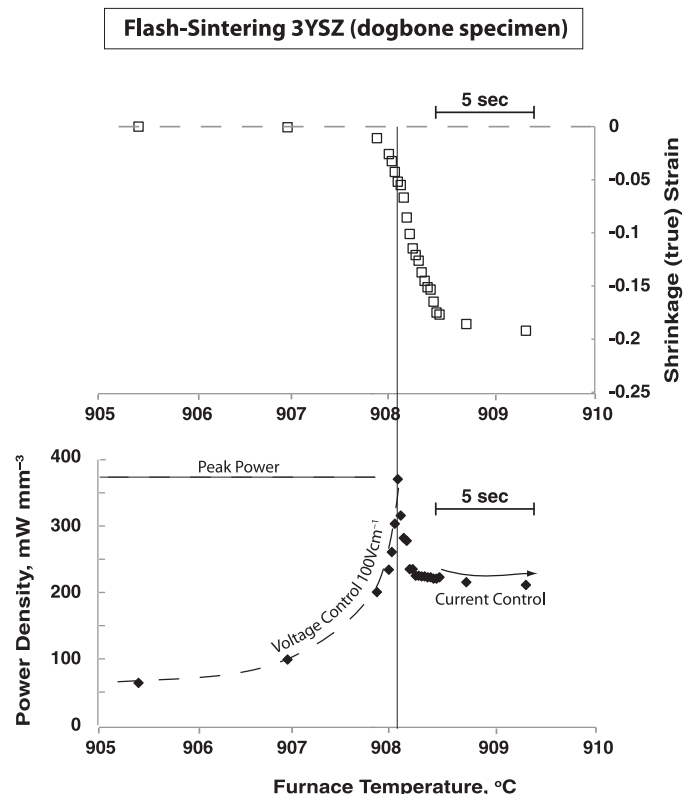


Fig. 4. The relationship between power density and sintering in the time domain in a flash-sintering experiment with 3YSZ. Data courtesy of M. Cologna.

MgO-alumina, but more than  $2000 \text{ mA mm}^{-2}$  for the case of cobalt-manganese oxide.

### 4. Extrapolation from conventional sintering

The absolute rates of sintering in flash sintering are very fast indeed, amounting to just a few seconds. In comparison conventional sintering needs an hour or more to achieve full density. Thus, the sintering rates are three to four orders of magnitude faster in flash-sintering as compared to conventional sintering. Here, assuming that the acceleration in sintering occurs from Joule heating of the specimen, we attempt to estimate how high the temperature must be in order to achieve accelerated sintering of this magnitude.

The Arrhenius form of the diffusion coefficient immediately leads to the following equation for establishing this relationship:

$$\log_{10} \frac{\text{Rate}_2}{\text{Rate}_1} = \frac{Q}{2.3R} \left( \frac{1}{T_1} - \frac{1}{T_2} \right) \quad (6)$$

where the subscript 1 refers to the temperature for conventional sintering, and subscript 2 corresponds to the higher rate at the higher temperature. Plots of Eq. (6) for three values of the activation energy,  $Q=400, 500, \text{ and } 600 \text{ kJ mol}^{-1}$ , are given in Fig. 5. These graphs permit a quick estimate of the temperature that would be required to accelerate the sintering rate by several orders of magnitude.

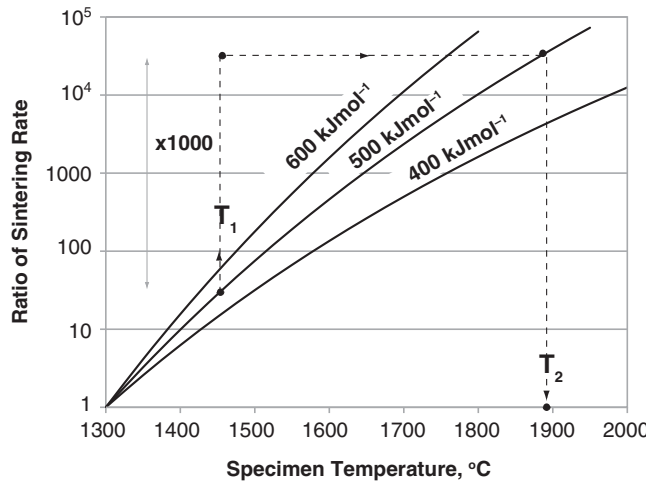


Fig. 5. The relationship between specimen temperature and the sintering rate for three different values of the activation energy for the coefficient for chemical diffusion. For example, a sample which sinters in an hour at 1400 °C, would require a temperature of 1800 °C to sinter in 3.6 s, assuming an activation energy of 500 kJ mol<sup>-1</sup>.

For example, assume that conventional sintering of 3YSZ requires 1 h at 1450 °C. We wish to estimate the temperature that would be needed to sinter in 3.6 s, that is, 1000 times faster. The graph shows that an increase in the sintering rate by a factor of 1000 would require a temperature of 1900 °C, if the activation energy is 500 kJ mol<sup>-1</sup>.<sup>10</sup>

As seen from the maps in Fig. 1, a power density of 400 mW mm<sup>-3</sup> at a furnace temperature of 900 °C would yield a specimen temperature of ~1250 °C, a difference of 350 °C. Even allowing that the black body model underestimates the specimen temperature by 200 °C, an upper bound value from comparisons presented earlier, the specimen temperature falls far short of 1900 °C that would be required from the Arrhenius extrapolation.

## 5. The heat capacity and the width of the power spike

The results in Figs. 3 and 4 show the power spike to have a width of approximately 1 s. Assuming a triangular shape of the spike, and the width at half maximum to be 1 s, the power expended in the specimen during this transient would be equal to  $\sim P_W^{\max} \times 1 \text{ mJ mm}^{-3}$ , where  $P_W^{\max}$  is expressed in units of mW mm<sup>-3</sup>. Even if the peak value is 1000 mW mm<sup>-3</sup>, the highest value seen in our experiments, the energy dissipated as heat in the specimen during this short period would be  $< 1 \text{ J mm}^{-3}$ . The question addressed here is what would be the increase in the specimen temperature as a result of this heat input into 3YSZ.

The density of zirconia is 5.7 g cm<sup>-3</sup>, and its heat capacity varies with yttria content and the phase of zirconia, but is generally in the range 75–85 J K<sup>-1</sup> mol<sup>-1</sup>. We shall assume a value of 80 J K<sup>-1</sup> mol<sup>-1</sup>, which translates into 0.65 J g<sup>-1</sup> K<sup>-1</sup> for the heat capacity for the molecular weight of 123 g mol<sup>-1</sup>. One mm<sup>3</sup> of zirconia weighs 0.0057 g mm<sup>-3</sup>, which then gives the following value for the heat capacity per unit volume: 0.004 J mm<sup>-3</sup> K<sup>-1</sup>.

It follows that heat dissipation of 1 J mm<sup>-3</sup>, with a heat capacity of 0.004 J mm<sup>-3</sup> K<sup>-1</sup> would give a temperature increase of

250 °C in the specimen, which is smaller than the temperature rise predicted from black body radiation. The inference is that the heat-dissipated during the power-spike in the flash experiments will be entirely consumed by the heat capacity of the material.

## 6. Conductivity as a function of temperature

In this section the behavior of the conductivity in the non-linear regime is analyzed. The results are from experiments with 8YSZ samples that had a density of 95%, achieved by conventional sintering.<sup>5</sup>

The above analysis is possible because the specimen was operated under current control. As shown in Ref. 6 a step-wise application of current to the specimen leads to a spike in the voltage generated across it, but which declines quickly to a steady state value. Since the voltage and the current applied to the specimen are now constant the sample is being supplied a constant level of power and a steady state in specimen temperature is established.

The specimen temperature was measured at different values of the steady state current. These data, therefore, permit the calculation of the specific resistivity of the specimen as a function of temperature. (These experiments were done under AC currents; the values for current density are the root mean square, RMS, values.)

The basic equations for the analysis are the current density,  $j$ , the electric field,  $E$ , the power dissipation per unit volume,  $W_V$ , and the specific resistivity,  $\rho$ . The following units for these parameters are used:

$$j \text{ mA mm}^{-2}, \quad E \text{ V cm}^{-1}, \quad W_V \text{ mW mm}^{-3}, \quad \rho \text{ Ohm cm} \quad (7)$$

They are related by the following equations:

$$W_V = \frac{E j}{10} \text{ mW mm}^{-3}, \quad \rho = \frac{10E}{j} \text{ Ohm cm}, \quad \text{and} \\ \rho = \frac{100W_V}{j^2} \text{ Ohm cm} \quad (8)$$

where the units given in Eq. (7) are applied to Eq. (8).

The author of Ref. 6 has kindly supplied the data for the current density, and the power density, and the specific resistivity of the specimens as a function of temperature, which are given as Table 1. The numbers show the resistivity to decrease by just a factor of ~2.5 when the temperature increases from 1275 °C to 1700 °C. An Arrhenius plot of these data in Fig. 6, gives an activation energy of 0.46 eV. Thus, in the “flash regime” the material behaves like a semiconductor with a small band gap.

The conductivity of YSZ under flash conditions, as discussed above, is almost certainly electronic, rather than ionic, for the following reasons:

- (i) The activation energy for the diffusion of oxygen ions in doped zirconia ranges up to 1.2 eV.<sup>11</sup> In the case of 8 mol%YSZ the activation energy ranges from 0.8

Table 1

The relationship between specimen temperature (as measured by thermal expansion) and its specific resistance.

Specimen temperature (°C)	Specific resistivity (Ohm cm)	Electrical field (V cm <sup>-1</sup> )	Current density (mA mm <sup>-2</sup> )
1224	4.71	8.8	19
1274	3.80	13.6	36
1341	3.25	17.4	54
1410	2.85	20.4	72
1476	2.55	22.6	89
1549	2.31	24.2	105
1589	2.10	25.1	120
1650	1.93	26.4	137

Courtesy: Guillon.<sup>5</sup>

to 1 eV.<sup>11,12</sup> Experimentally, the activation energy has been found to increase with increasing yttria content.<sup>11</sup> However, the activation energy declines with increasing temperature which is attributed to the aggregation of defects.<sup>13</sup> Since the experiments for oxygen ion diffusion are usually conducted in the 300–1000 °C range, one can question how low the value of the activation energy may be at much higher temperatures. But the activation energy cannot be lower than the value for hopping energy for oxygen ions, which has been calculated to be 0.63 eV,<sup>14</sup> still higher than the measured value of 0.46 eV.

(ii) High current of oxygen ions through the specimen would lead to reduction of zirconium oxide at the cathode into zirconium metal, which we do not find.

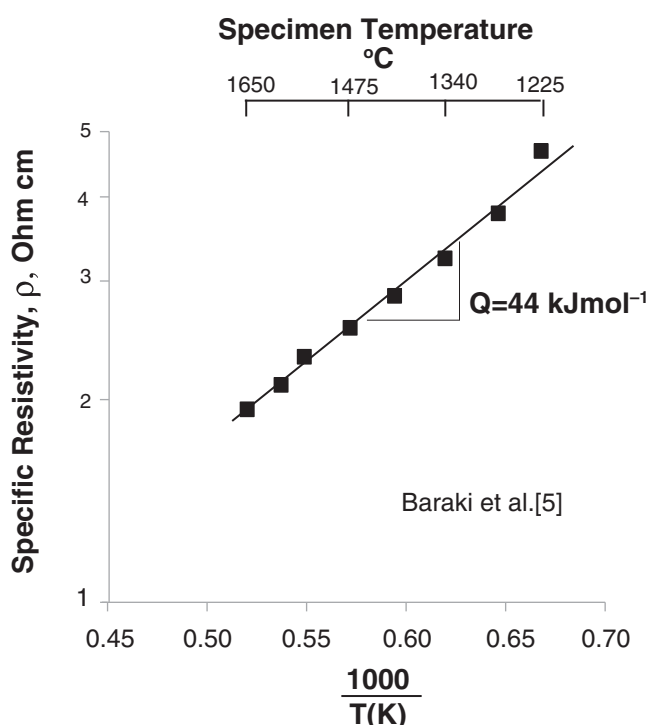


Fig. 6. An Arrhenius plot of the specific resistivity of the specimen as a function of the temperature. The full data are tabulated in Table 1.  
Data courtesy of Olivier Guillon.

(iii) We have observed that the anode where oxygen ions oxidize into oxygen heats up due to the high electrode-interface resistance arising from the release of oxygen. However, upon entering the flash regime, the electrode immediately cools, which is explained by a transition to electronic conduction which renders the metal-electrodes to become non-blocking.

## 7. Discussion

The phenomenon of flash sintering has an important characteristic: the onset of rapid sintering is accompanied by a highly non-linear increase in the conductivity of the specimen. The dichotomy in understanding the underlying mechanism arises from the difference in the fundamental nature of electrical conductivity, which is controlled by the fastest moving charged species, and sintering, where mass transport is controlled by slowest moving charged species.

This dichotomy may be resolved by Joule heating. The argument being that the rise in temperature arising from Joule heating, produced by the sudden increase in electrical conductivity, increases the rate of chemical diffusion. If the power density exceeds 1000 mW mm<sup>-3</sup> then it is conceivable that specimen temperatures of up to 1800 °C can be reached which could be high enough to explain the sintering of YSZ specimens in just a few seconds.

However, the flash sintering experiments do not endure such high power densities in a sustained way. While the peak value of the power-spike can be high, the steady state power density, once the spike has passed, is far lower. The spike occurs because the power supply is switched from voltage control to current control to avoid electrical runaway. Under current control the power declines as the resistance of the specimen continues to fall. The steady state power dissipation regime is approximately 125–200 mW mm<sup>-3</sup>. These levels of power dissipation are unlikely to produce temperatures that would be required to achieve sintering in a few seconds.

What then may be the mechanism for explaining flash-sintering? The onset of the flash phenomenon is related not only to the temperature but also to the electrical field. In the flash regime the specimens become electronically conducting. The production of Frenkel pairs and their ionization under the electric field has been proposed to explain the increase both the electrical conductivity and the mass transport.<sup>15</sup>

There remains the question to what extent Joule heating contributes to flash-sintering. The specimen temperature, though several degrees higher than the furnace temperature, remains well below the temperature that would be required to densify in just a few seconds. Therefore, we infer that sintering kinetics is enhanced by the production of defects, as discussed just above. The important question to ask is how Joule heating contributes to the mechanism of defect production.

It is interesting to note that in oxides of different chemistries, ionic and electronic conductivities, and stoichiometry,<sup>1–4</sup> the power dissipation in the flash-regime usually falls in the

100–400 mW mm<sup>-3</sup> range, even though the threshold values of field and temperature, for the flash-transition, vary greatly. This observation raises the question if local heating at grain boundaries is precipitating the instability; this explanation can be explored by studying the influence of the grain size, even extending to single crystals, on the flash-transition.

Recent works on “flash welding” of YSZ powders shows effects similar to those seen in flash sintering.<sup>16,17</sup> There is a large increase in conductivity above a threshold applied field, and the resistance of the specimen declines thereafter. The authors attributed these observations to Joule heating.

The influence of an electric field on the tensile superplastic deformation of oxides has been studied by Conrad and co-workers.<sup>18</sup> They report significant drops in the flow stress, which they partition into three components: the first arising from Joule heating, the second being linked to the immediate influence of the field on transport kinetics since the flow stress is seen to fall and rise as the field is turned on and off, and the third being related to the cumulative influence of the applied field on the microstructure – principally grain growth – during the experiment. The large effect seen in the on-off experiments with MgO-doped alumina are particularly noteworthy. In view of the very high furnace temperatures in these experiments it is possible that the samples were being operated in the high conductivity regime (while the fields used in the deformation experiments were lower than those in flash sintering of MgO-Al<sub>2</sub>O<sub>3</sub>, the furnace temperatures were much higher; the critical field for the flash event declines as the furnace temperature rises). Measurements of the power density would serve to clarify this point.

## 8. Conclusions

Flash sintering of several oxides is invariably accompanied by a sudden increase in the conductivity of the specimen. This observation requires a mechanism that can explain a simultaneous increase in electrical conductivity and mass transport kinetics. However, the first is controlled by the fastest moving, and the latter by the slowest moving charged species.

Joule heating of the specimen is a simple way to explain this coupling between charge and mass transport. The transient nature of the flash-sintering process, however, requires care in estimating the specimen temperature. The increase in conductivity produces a surge in power dissipation when a constant voltage is applied to the specimen. The power supply switches to current control when the power reaches a preset value, which causes the power dissipation to decline and finally approach a steady state. The analysis of the this power spike shows that specimen temperature is determined not by the peak value of the spike, but by the steady state value of the power dissipation in the current controlled regime. The measurement of specimen temperature agrees with these estimated values.

While the specimen temperature rises a few hundred degrees above the furnace temperature, it remains several hundred

degrees below the temperature that would be required to sinter the specimen in a few seconds.

Therefore, Joule heating, by itself, cannot explain the phenomenon of flash-sintering. It is proposed that the applied field and the higher specimen temperature act synergistically to produce an avalanche of defects, such as Frenkel pairs, that greatly enhance the rate of mass transport.

## Acknowledgements

This work was supported by the Basic Energy Sciences Division of the Department of Energy under Grant No.: DE-FG02-07ER46403. Valuable inputs from Prof. F. Wakai, of the Tokyo Institute of Technology are greatly appreciated. I sincerely thank Professor O. Guillot of the Friedrich-Schiller University, Germany, for not only providing thoughtful feedback to the manuscript, but also the data that is included in Table 1. Finally my gratitude to Marco Cologna and John S.C. Francis goes without saying. What is in here is a direct result of their innovative research on this topic. This manuscript was prepared while the author was visiting the Tokyo Institute of Technology, Sukukakedai Campus, as a JSPS fellow.

## References

- Cologna M, Rashkova B, Raj R. Flash sintering of nanograin zirconia in <5 s at 850 °C. *J Am Ceram Soc* 2010;93(11):3557–9.
- Cologna M, Prette ALG, Raj R. Flash-sintering of cubic yttria-stabilized zirconia at 750 °C for possible use in SOFC manufacturing. *J Am Ceram Soc* 2011;94(2):316–9, doi:10.1111/j.1551-2916.2010.04267.x.
- Cologna M, Francis JSC, Raj R. Field assisted and flash sintering of alumina and its relationship to conductivity and MgO-doping. *J Eur Ceram Soc* 2011;31(11):2827–37, doi:10.1016/j.jeurceramsoc.2011.07.004.
- Karakuscu A, Cologna M, Yarotski D, Won J, Raj R, Überuaga BP. Defect structure of flash sintered strontium titanate. *J Am Ceram Soc*; under review.
- Baraki R, Schwarz S, Guillot O. Effect of electrical field/current on sintering of fully stabilized zirconia. *J Am Ceram Soc* 2012;95(1):75–8, doi:10.1111/j.1551-2916.2011.04980.x.
- Grasso S, Sakka Y, Rendtroff N, Hu C, Maizza V, Borodianska H, et al. Modeling of the temperature distribution of flash sintered zirconia. *J Ceram Soc Jpn* 2011;119(2):144–6.
- Francis JSC, Raj R. Flash-sinterforging of nanograin zirconia: field assisted sintering and superplasticity. *J Am Ceram Soc* 2011, doi:10.1111/j.1551-2916.2011.04855.x, published online.
- Cologna M, Raj R. Surface diffusion-controlled neck growth kinetics in early stage sintering of zirconia, with and without applied DC electrical field. *J Am Ceram Soc* 2010;94(2):391–5, doi:10.1111/j.1551-2916.2010.04088.x.
- Yang D, Raj R, Conrad H. Enhanced sintering rate of zirconia (3Y-TZP) through the effect of a weak dc electric field on grain growth. *J Am Ceram Soc* 2010;93(10):2935–7, doi:10.1111/j.1551-2916.2010.03905.x.
- Wakai F, Sakaguchi S, Matsuno Y. Superplasticity of yttria-stabilized tetragonal ZrO<sub>2</sub> polycrystals. *Adv Ceram Mater* 1986;1(3):259–63.
- Devanathan R, Weber WJ, Singhal SC, Gale JD. Computer simulation of defects and oxygen transport in yttria-stabilized zirconia. *Solid State Ionics* 2006;177:1251–8, doi:10.1016/j.ssi.2006.06.030.
- Gonzales-Romero RL, Melendez JJ, Gomez-Garcia D, Cumbrera FL, Dominguez-Rodriguez A, Wakai F. *Solid State Ionics*; doi:10.1016/j.ssi.2011.10.006, in press.
- Badwal SPS. Electrical conductivity of single crystal and polycrystalline yttria-stabilized zirconia. *J Mater Sci* 1984;19:1767–76.
- Mackrodt WC, Woodrow PM. Theoretical estimates of point defect energies in cubic zirconia. *J Am Ceram Soc* 1986;69(3):277–80.

15. Raj R, Cologna M, Francis JSC. Influence of externally imposed and internally generated electrical fields on grain growth, diffusional creep, sintering and related phenomena in ceramics. *J Am Ceram Soc* 2011;94(7):1941–65, doi:10.1111/j.1551-2916.2011.04652.x.
16. Muccillo R, Kleitz M, Muccillo ENS. Flash grain welding in yttria stabilized zirconia. *J Eur Ceram Soc* 2011;31:1517–21.
17. Cordier A, Kleitz M, Steil C. Welding of yttrium-doped zirconia granules by electric current activated sintering, *J Eur Ceram Soc*; in review.
18. Conrad H, Yang D. Influence of an applied DC electric field on the plastic deformation kinetics of oxide ceramics. *Philos Mag* 2010;90(9):1141–57, doi.org/10.1080/14786430903304137.